



Effect of Eccentricity Factors on End Winding Electromagnetic Force in Turbo-generator

Hong Chun Jiang, Yu Ling He*, Gui Ji Tang

Hebei Key Laboratory of Electric Machinery and Failure Prevention, North China Electric Power University, Baoding, China

Email address:

heyuling1@163.com (Yu Ling He)

*Corresponding author

To cite this article:

Hong Chun Jiang, Yu Ling He, Gui Ji Tang. Effect of Eccentricity Factors on End Winding Electromagnetic Force in Turbo-generator.

International Journal of Electrical Components and Energy Conversion. Special Issue: *Electro-Mechanical Coupling Problems in Electric Machines*. Vol. 7, No. 2, 2021, pp. 48-53. doi: 10.11648/j.ijecec.20210702.13

Received: October 28, 2021; **Accepted:** November 19, 2021; **Published:** November 27, 2021

Abstract: Static eccentricity will cause the abnormal distribution of air gap magnetic field and further affect the electromechanical characteristics of the generator. This paper comparatively studies on the end winding electromagnetic force of turbo generator under different eccentricity ratio and eccentricity angle. The analytical expression of end winding electromagnetic force is derived after eccentricity. Meanwhile, the three-dimensional transient finite element simulation is carried on under several eccentricity cases. Then the amplitude variation characteristics with eccentricity ratio and angle are analyzed. Further, the force characteristics are verified by experimental vibration acceleration of CS-5 simulating generator. It is found that the static eccentricity will not change the frequency components of the end winding force. However, it will change the amplitude of the electromagnetic force, and the increase or decrease tendency depends on the winding position, eccentricity ratio and eccentricity angle. The number of force amplitude increasing coils is close to half of the total number, and it changes slightly with the eccentricity ratio and eccentricity angle. The force increment of coil near the minimum air gap will be larger with the increase of eccentricity ratio, but it is not affected greatly by eccentricity angle. Moreover the coil with the most obvious force increase is located in the interphases position near the minimum air gap.

Keywords: Electromagnetic Force, Eccentricity Factors, End Winding, Turbo-generator

1. Introduction

Static air gap eccentricity refers to the offset between rotor and stator axis, and it is a common mechanical fault of generator. Due to machining and installation errors, almost all generators have a static eccentricity with different extents. Especially for large turbo generator, because its shafting supporting component is sliding bearing, static air gap eccentricity is inevitable. This fault will not seriously affect the operation of the unit when they are slight in the early stage, and the generator can still run for a long time, so it is often ignored. However, static eccentricity will cause the abnormal distribution of air gap magnetic field and further affect the electromechanical characteristics of the generator.

When the rotor is eccentric, the magnetic field will be deformed [1-4]. Further, the unbalanced magnetic pull of the rotor will increase, and its direction will shift with the change of eccentricity angle. Radial eccentricity will increase the

harmonic amplitude of the electromagnetic torque, while axial eccentricity is the opposite [5, 6]. In addition, it is pointed out that, under eccentricity, the electromagnetic force of winding line part increases where the air gap length is shorter, and it decreases where the air gap length is longer [7-8]. Meantime, eccentricity will increase the characteristic frequency amplitude of stator current, and Liu Fei proposed an eccentricity detection method based on current signal [9]. Based on the above, the eccentricity detection methods are summed from the four aspects of voltage/current harmonic components, efficiency, temperature and electromagnetic torque fluctuation [10].

Moreover, the air gap eccentricity will also affect the electromagnetic force of the stator end winding. And it further influent the vibration wear of the end winding [11], because the end part of stator winding is suspended outside

the stator slot, as shown in Figure 2b). However, in the existing literature, there are few studies on the electromagnetic force and vibration characteristics of stator end winding under air gap eccentricity fault. In the study of Hong-Chun Jiang et al. [12], we found that the vibration and wear of the coil near the minimum air gap will increase under a particular eccentric ratio and angle. As an improvement, this paper mainly studies on the variation characteristics of the electromagnetic force with different eccentricity ratio and angle.

The remainder of this paper is constructed as follows. The qualitative equation of the end winding electromagnetic force under eccentricity is derived in Section 2. Then, the finite element analysis is carried out in Section 3. Further, the force characteristics are experimentally verified by vibration acceleration in Section 4. Finally, the main conclusions are drawn up in Section 5.

2. Theoretic Analysis

According to Hong-Chun Jiang et al. [12], the magnetic flux force (MMF) of the stator windings, rotor windings and summed MMF can be written as

$$\begin{cases} f_s(\alpha, t) = \sum_{n=1,3,5,\dots} F_{sn} \cos[n(\omega t - \alpha p) - \psi - 0.5\pi] \\ f_r(\alpha, t) = \sum_{n=1,3,5,\dots} F_{rn} \cos n(\omega t - \alpha p) \\ f(\alpha, t) = \sum_{n=1,3,5,\dots} F_{cn} \cos n(\omega t - \alpha p - \rho_n) \end{cases} \quad (1)$$

where α is the circumferential position, p is the number of pole pair, ψ is the internal power angle of generator, ω is the electricity frequency, F_{sn} , F_{rn} and F_{cn} is the n -th harmonics amplitude of stator windings, rotor windings and summed MMF, respectively. ρ_n is the angle between the rotor winding MMF and summed MMF vectors.

When the static eccentricity happens, the permeance will be varied. The permeance in unit area can be expressed as [13]

$$\Lambda(\alpha) = \frac{\mu_0}{\delta(\alpha)} = \frac{\mu_0}{\delta_0 [1 - \zeta \cos(\alpha - \lambda)]} \approx \Lambda_0 [1 + \zeta \cos(\alpha - \lambda)] \quad (2)$$

Where $\delta(\alpha)$ represents the air gap length of different circumferential position, Λ_0 refers to the normal permeance ($\Lambda_0 = \mu_0/\delta_0$, μ_0 and δ_0 are the vacuum permeability and normal air gap length, respectively), ζ is the relative eccentricity ratio ($\zeta = e/\delta_0$, e is the absolute eccentricity value), and λ is the eccentricity angle as shown in Figure 1.

The air-gap MFD can be obtained by the multiplication of the unit permeance under eccentricity and the MMF in normal condition.

$$\begin{aligned} B_e(\alpha, t) &= f(\alpha, t) \Lambda(\alpha) \\ &= \Lambda_0 [1 + \zeta \cos(\alpha - \lambda)] \sum_{n=1,3,5,\dots} F_{cn} \cos n(\omega t - \alpha p - \rho_n) \quad (3) \\ &\approx \Lambda_0 [1 + \zeta \cos(\alpha - \lambda)] F_{c1} \cos(\omega t - \alpha p - \rho_1) \end{aligned}$$

It can be indicated from equation (3) that when the air gap is statically eccentric, the MFD will increase near the minimum air gap and decrease near the maximum air gap. The frequency component after eccentricity is the same as normal condition, and it still contains only odd harmonic components.

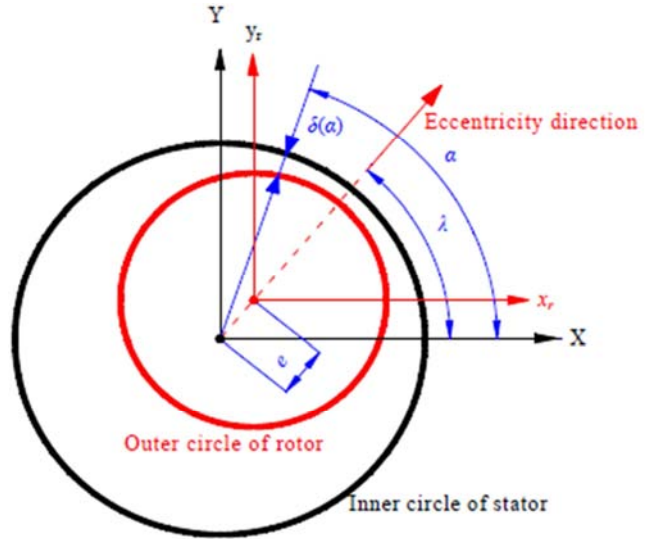


Figure 1. Diagram of air-gap static eccentricity.

Using ampere force law, MFD after eccentricity and stator winding current (details see Ref. [12]), the expression of electromagnetic force at point K of end winding can be deduced as Eq. (4). F_{Ikxe} , F_{Ikze} and F_{Ikze} are the rectangular coordinate components of electromagnetic force under eccentricity, B_e and I_e is the air gap MFD of line part and stator current respectively. f_k is the decrease factor of end zone magnetic field, F_{Ike} and F_{Ik} is electromagnetic force in normal and eccentricity respectively. θ_k is the angle between the MFD and the stator current at Point K . α_l is the circumferential angle of the upper layer line part in the l -th stator slot, and $\alpha_r + \alpha_k$ refers to position of the point K as shown in Figure 2 (a).

According to equation (4), when the air gap is statically eccentric, the frequency component of the electromagnetic force is the same as normal condition, and it includes constant component and even harmonics. Although the static eccentricity does not affect the frequency composition of the electromagnetic force, it will change the amplitude of the end winding electromagnetic force, and the increase or decrease tendency Δ depends on the winding position, eccentricity ratio and eccentricity angle.

$$\begin{cases}
\overline{F_{lke}} = f_k \overline{B_e} \times \overline{I_e} dl = \{\overline{F_{lke}}, \overline{F_{lkye}}, \overline{F_{lkze}}\} dl \\
F_{lke}(\alpha_l + \alpha_k, t) = f_k B_e I_e \sin \theta_k dl \\
= \frac{pqdl}{a|Z|} f_k w_s L v \Lambda_0^2 \sin \theta_k [1 + \zeta \cos(\alpha_l + \alpha_k - \lambda)][1 + \zeta \cos(\alpha_l - \lambda)] \\
\sum_{n=1,3,5,\dots} \sum_{j=1,3,5,\dots} k_{wn} F_{rn} F_{cj} \cos p[(n+j)(\omega t - \alpha_l) - j\alpha_k - j\rho_n / p - \psi - 0.5\pi] \\
+ \cos p[(n-j)(\omega t - \alpha_l) - j\alpha_k - j\rho_n / p + \psi + 0.5\pi] \\
= (1 + \Delta) F_{lk} \\
\Delta = \zeta^2 \cos(\alpha_l + \alpha_k - \lambda) \cos(\alpha_l - \lambda) + \zeta \cos(\alpha_l + \alpha_k - \lambda) + \zeta \cos(\alpha_l - \lambda) \\
\approx \zeta \cos(\alpha_l + \alpha_k - \lambda) + \zeta \cos(\alpha_l - \lambda)
\end{cases} \quad (4)$$

3. Finite Elementary Calculation

In this section, the end winding electromagnetic force of QFSN-600-2YHG turbo generator under static air gap eccentricity are simulated and calculated. The specific parameters of generator can be obtained in the research of Hong-Chun Jiang *et al.* [12]. The stator winding distribution is shown in Figure 2.

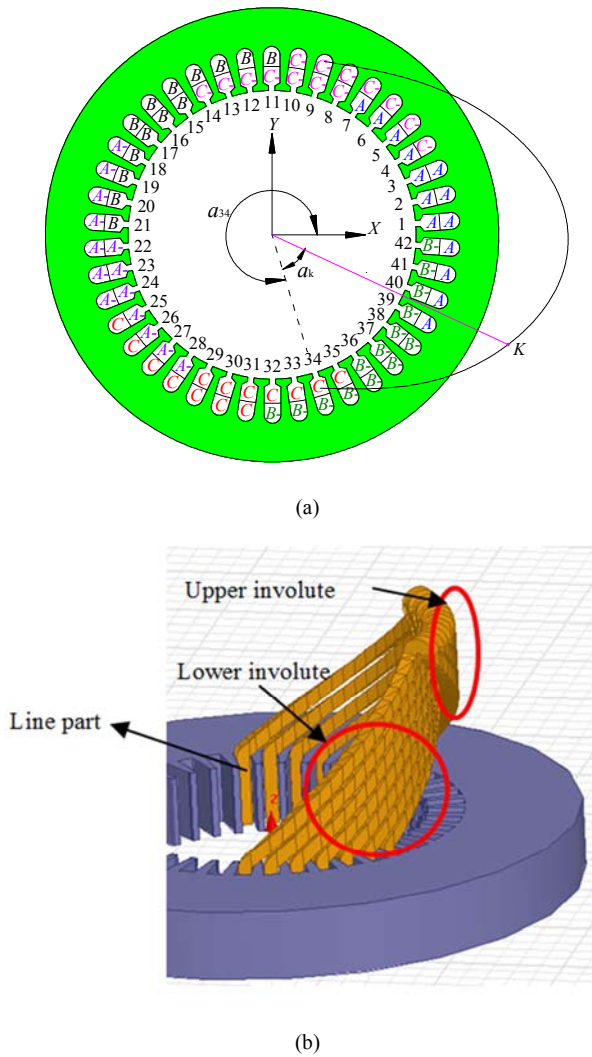


Figure 2. Stator windings: (a) Section view, and (b) 3D view.

3.1. Line Part MFD

When the eccentricity is 0.3 and the eccentricity angle is 0° , the radial MFD wave and its spectrum at the minimum air gap are shown in Figure 3. It can be seen from Figure 3 a) that the MFD wave still approximately matches in cosine with time after eccentricity. As the air gap length decreases at 0° position, its magnetic permeance will increase (see Eq. (2)), and the MFD peak value becomes larger. Moreover, it shows in Figure 3 b) that the MFD after static eccentricity still contains obvious 50Hz frequency component (that is the fundamental frequency ω), weak 150Hz and 250Hz (that is 3ω and 5ω). This conclusion is consistent with the conclusion from Eq. (3) in theoretical analysis.

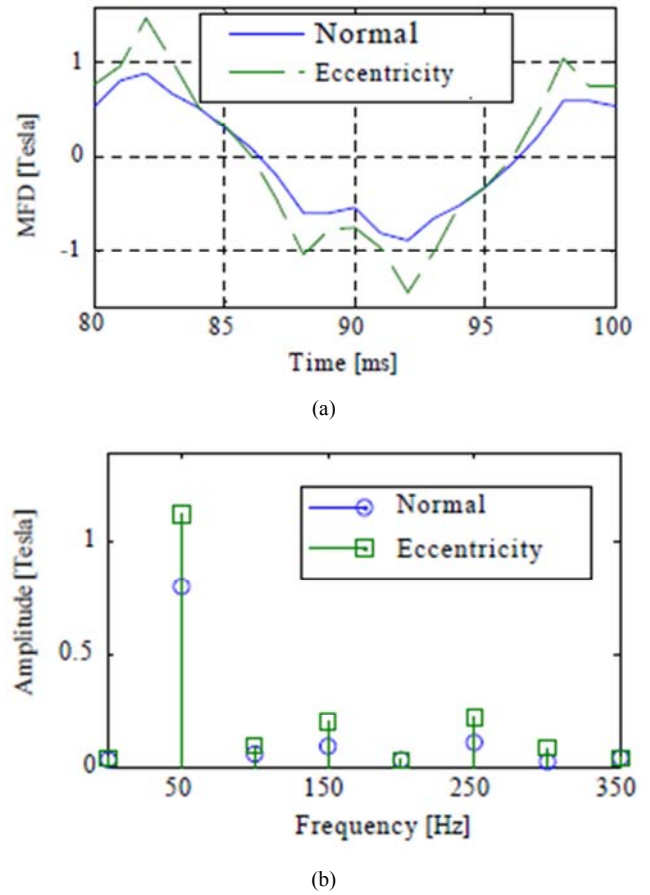


Figure 3. Radial flux density: (a) Time wave, (b) Spectrum.

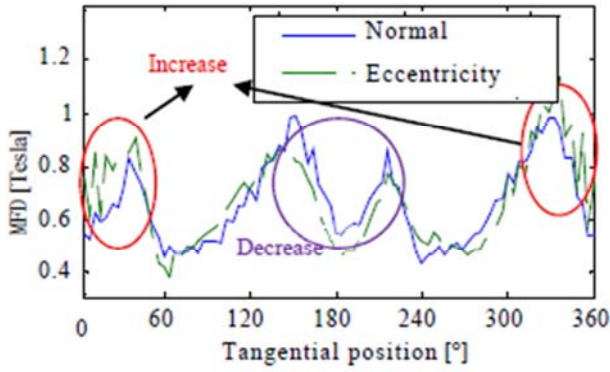


Figure 4. Air-gap flux density distribution.

When $t=100\text{ms}$, the distribution curve of the comprehensive MFD along the circumferential direction is shown in Figure 4. Due to the change of the radial air-gap length, the magnetic density increases near 0° after eccentricity, while it decreases near 180° .

3.2. Electromagnetic Force of End Winding

Figure 5 shows the time domain wave and spectrum of coil 34 electromagnetic force when static eccentricity ratio is 0.3 and eccentricity angle is 0° .

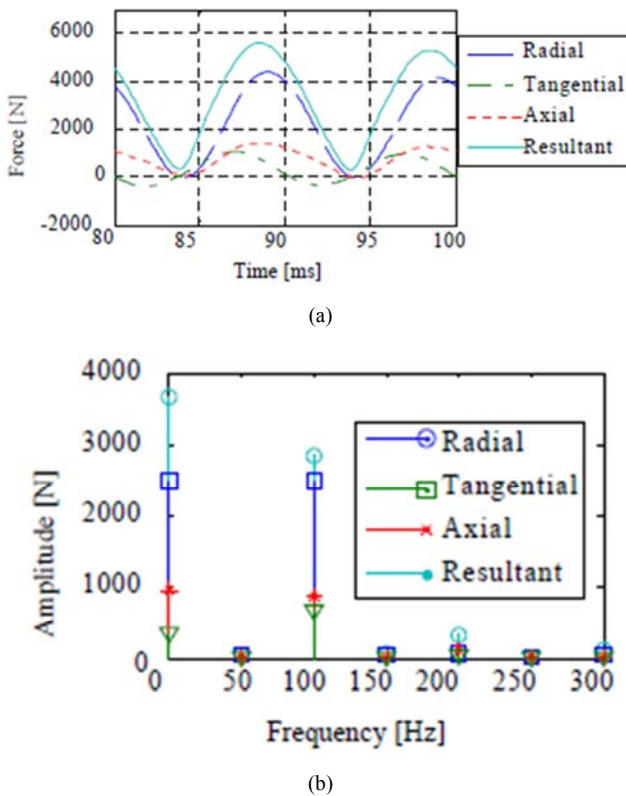


Figure 5. Electromagnetic force and spectrum of Coil 34 end part: (a) Time wave, (b) Spectrum.

The frequency component of the force contains obvious DC constant, 100Hz component (that is 2nd harmonic) and weak 200Hz component (that is 4th harmonic). This result is consistent with the theoretical analysis result of Eq.(4). In

addition, since the circumferential electromagnetic force is the difference for two involutes (see Figure 8 a) in [14]), it has little significance for the analysis of vibration wear. The number of force increase coil for axial direction is wider than radial direction (see Figure 6 a) and b) in [12]). Therefore, the influence of eccentricity ratio and eccentricity angle on the second harmonic of end winding vibration is analyzed through axial force.

(1) Eccentricity ratio effect

The 2nd harmonic amplitude of axial electromagnetic force on each coil under different eccentricity ratio is shown in Figure 6. As is shown, the force amplitude increment is enlarged with the increasing of eccentricity ratio. The number of coils with increased amplitudes is close to half of all, and it will change slightly with the eccentricity ratio. During the normal operation, the force amplitude of the interphase coil is the largest, and the vibration and wear are serious. When the eccentricity is 0.1, the force amplitudes of coils 28, 29, 30, 33-36, 41 and 42 exceed the normal interphase coils, and the force amplitude of coils 7, 14 and 21 decreases. When the eccentricity reaches 0.2, the electromagnetic force amplitude of 27-42 coils exceeds the normal interphase coils, that is, 1/3 of the total coils are under serious vibration. When the eccentricity reaches 0.3, the number of coils that exceed the normal interphase coils is basically the same as that when the eccentricity is 0.2, but the amplitude of coils 29, 34 and 35 increases to the 120% of the normal value, and the corresponding vibration and wear degree will also be enlarged. So, the force increment becomes great with the increase of eccentricity ratio.

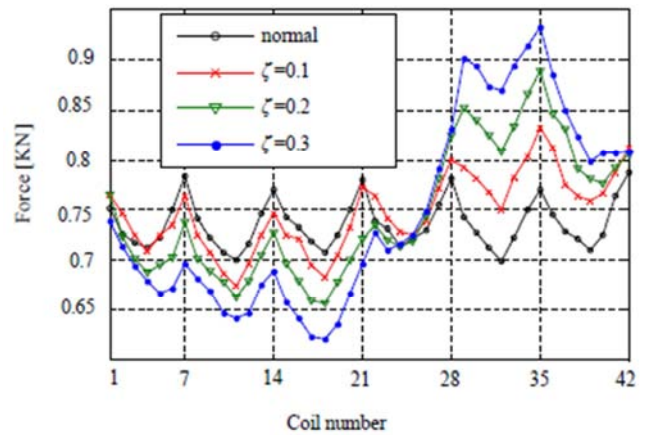


Figure 6. Second harmonic amplitude of electromagnetic force under different eccentricity ratios.

(2) Eccentricity angle effect

It can be seen from Eq. (4) that when the eccentricity angle difference is 60° , the force influences on the two coils which are 60° apart are the same. For example, when the eccentricity angle is 0° , the change of electromagnetic force amplitude of coil 35 is basically the same as coil 42 when the eccentricity angle is 60° . Therefore, in order to study the influence of eccentricity angle, it is only necessary to analyze the situation when the eccentricity angle is 0° to 60° .

When the eccentricity ratio is 0.2 and the eccentricity angle is 0° , 20° and 40° , the 2nd harmonic amplitude of the axial electromagnetic force on each coil is shown in Figure 7. As is shown, the number of force amplitude increasing coils in the three cases is 17, 19 and 24 respectively, and they are close to half of the total number. These coil numbers are (27-42, 1), (28-42, 1-4) and (28-42, 1-9). The centre position of these coil groups is 4° , 28° and 47° respectively, so it moves with the change of eccentricity angle.

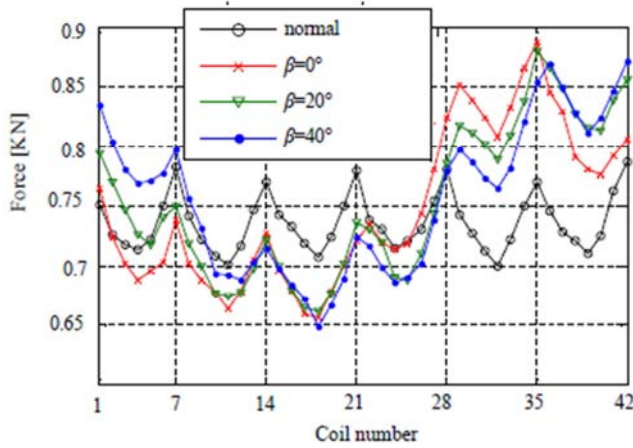


Figure 7. Second harmonic amplitude of electromagnetic force under different eccentricity position.

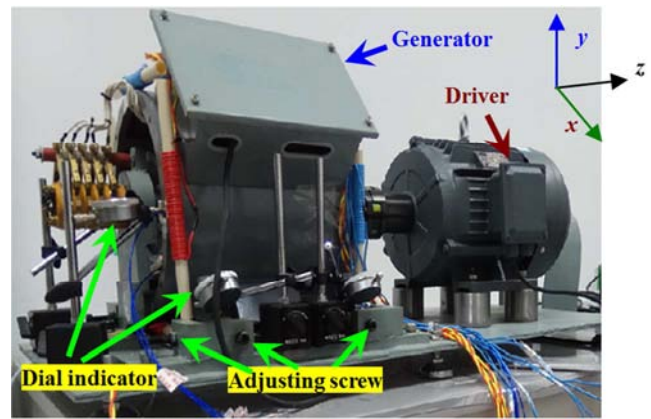
Though the number of force amplitude increasing coils changes slightly with the eccentricity angle, they are mostly concentrated in coils 28-42. That is to say, the vibration and wear of two-phase coils near the minimum air gap will increase. The three eccentricity angles are the centres of coil 34, 36 and 39 respectively, and the interphase coils near the three coils are 35, 35, 36 and 42 respectively. Therefore, the amplitude of coil 35 is the largest when the eccentricity angle is 0° and 20° , and it is 14% and 13% higher than the normal condition respectively. When the eccentricity angle is 40° , the amplitude of coils 36 and 42 is the largest, which is 12% higher than the normal condition. It indicates that the vibration and wear of interphase coils near the minimum air gap will be intensified, and the aggravation degree is not greatly affected by the eccentricity angle.

4. Experimental Study

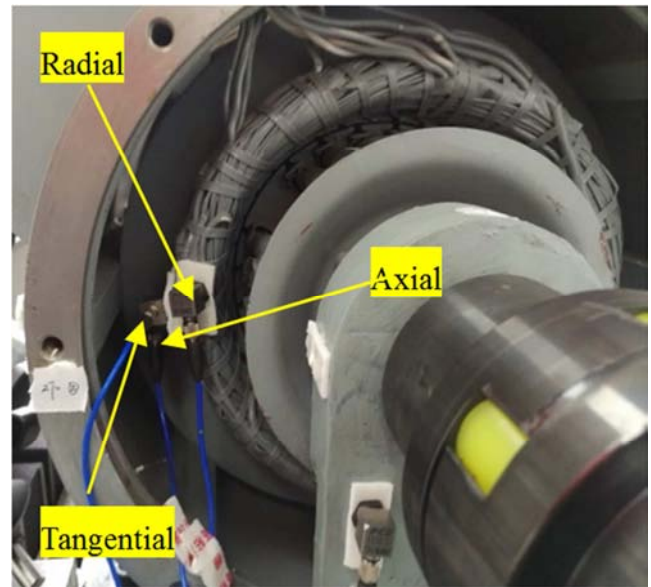
The end vibration is the response to the electromagnetic force, there is the frequency relation between the force and vibration. So, in this section, the above force characteristics of the end winding are verified by experimental vibration acceleration on CS-5 fault simulator. The electrical frequency of the generator is 50Hz. During the experiment, the

acceleration sensors are pasted on the end winding through double-sided adhesive tape, as shown in Figure 8 b). Moreover, the normal radial air-gap is 1.2mm, and its value is decreased by 0.12mm and 0.18 in the eccentric experiment. And the eccentricity value is controlled by two dial indicators as shown in Figure 8 a).

The experimental acceleration spectrum at the min air gap is shown in Figure 9. It indicates in the figure that the acceleration contains obvious harmonics at 100Hz and 200Hz. Besides, there are components at 50Hz and 150Hz, and they are the rotor rotating frequency and support natural frequency. With the eccentricity ratio increasing, the acceleration amplitude at 100Hz and 200Hz is becoming larger. And this result is consistent with the simulated force of coil 34 in Figure 6.



(a)



(b)

Figure 8. CS-5 fault simulation generator: (a) Prototype generator, (b) Sensor layout.

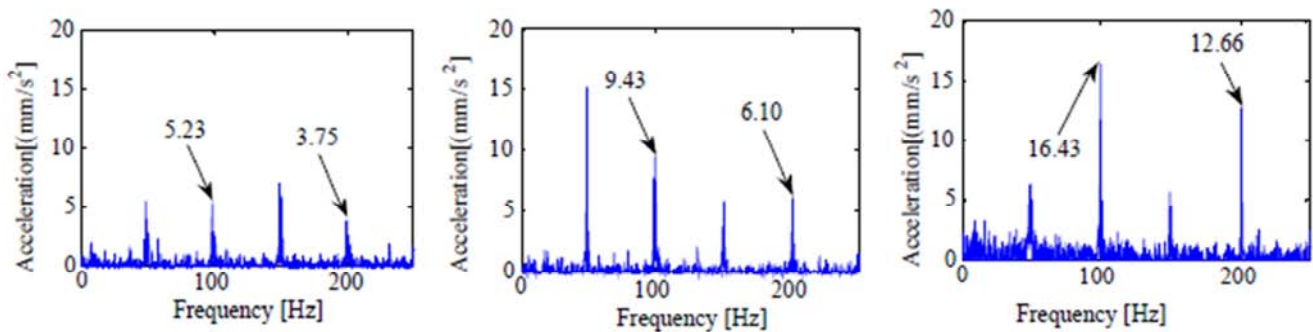


Figure 9. Axial vibration acceleration: (a) Normal, (b) Eccentricity $\zeta=10\%$, and (c) eccentricity $\zeta=15\%$.

5. Conclusion

In this paper, the electromagnetic force of stator end winding are comparatively analysed under different eccentricity ratio and eccentricity angle. It is found that the number of force amplitude increasing coils is close to half of the total number, which changes slightly with the eccentricity ratio and angle. The increment of coil near the minimum air gap will be larger with the increase of eccentricity ratio, but it is not affected greatly by eccentricity angle. Moreover, the coil with the most obvious force increase is located the interphase position near the minimum air gap.

Acknowledgements

This work is supported by the National Natural Science Foundation of China (51777074) and the fundamental research funds for central universities (2017MS146).

References

- [1] B. A. T. Iamamura, Y. Le Menach, A. Tounzi, N. Sadowski, et al. "Study of Static and Dynamic Eccentricities of a Synchronous Generator Using 3-D FEM," *Transactions on Magnetics*, vol. 46, no. 8, pp. 3516–3519, 2010.
- [2] Zhang, Guoyuan; Wei, Junchao; Huang, Haizhou; Zhou, Miao. "A study on the nonlinear vibration of the generator rotor based on the unbalanced electromagnetic force and the oil film force coupling model," *Journal of Vibroengineering*, vol. 15, no. 1, pp. 23-36, 2013.
- [3] C. Patsios, A. Chaniotis, E. Tsampouris and A. Kladas. "Particular Electromagnetic Field Computation for Permanent Magnet Generator Wind Turbine Analysis," *IEEE Transactions on Magnetics*, vol. 46, no. 8, pp. 2751-2754, 2010.
- [4] Y. He et al. "A New External Search Coil Based Method to Detect Detailed Static Air-Gap Eccentricity Position in Non-Salient Pole Synchronous Generators", *IEEE Transactions on Industrial Electronics*, pp. PP (99): 1-1, 2020, doi: 10.1109/TIE.2020.3003635.
- [5] Y. He et al. "Effect of 3D Unidirectional and Hybrid SAGE on Electromagnetic Torque Fluctuation Characteristics in Synchronous Generator," *IEEE Access*, vol. 7, pp. 100813-100823, 2019.
- [6] Y. He et al. "Rotor UMP characteristics and vibration properties in synchronous generator due to 3D static air-gap eccentricity faults," *IET Electric Power Applications*, vol. 14, no. 6, pp. 961-971, 2020.
- [7] Yan Xuechao. "Analysis of Magnetic Field and Calculation of Magnetic Force for Large Turbo-generator with Rotor Eccentricity," Harbin University of Science and Technology, Harbin, China, 2013 (in Chinese).
- [8] Zhang Wenzhan. "Analysis and application of electromagnetic force on turbo-generator rotor and stator", North China Electric Power University, Hebei, Chian, 2010 (in Chinese).
- [9] Liu Fei, Liang Lin, Xu Guanghua, Dong Jiacheng. "A Detection Method of Motor Rotational Eccentricity Using Current Information," *Transactions of China Electrotechnical Society*, vol. 29, no. 7, pp. 181-186+208., 2014 (in Chinese).
- [10] H. Ehya, I. Sadeghi and J. Faiz. "Online condition monitoring of large synchronous generator under eccentricity fault," 2017 12th IEEE Conference, 2017.
- [11] J. A. Tegopoulos, "Forces on the End Winding of Turbine-Generators II - Determination of Forces" *IEEE Transactions on Power Apparatus and Systems*, 1966, 85 (2): 14-122.
- [12] Hong-Chun Jiang, Gui-Ji Tang, Yu-Ling He et al., "Effect of Static Rotor Eccentricity on End Winding Forces and Vibration Wearing," *International Journal of Rotating Machinery*, vol. 2021, pp. 1-14, 2021.
- [13] Yu-Ling He, Wei-Qi Deng, Bo Peng, etc. "Stator Vibration Characteristic Identification of Turbogenerator among Single and Composite Faults Composed of Static Air-Gap Eccentricity and Rotor Interturn Short Circuit" *Shock and Vibration*, vol. 2016, pp. 1-14, 2016.
- [14] H.-C. Jiang, Y.-L. He, G.-J. Tang, and M.-X. Xu, "A comprehensive analysis on transient electromagnetic force behavior of stator windings in turbo-generator," *Mathematical Problems in Engineering*, vol. 2018, pp. 1-16, 2018.